



Machine vision system for classification of bulk raisins using texture features

Mostafa Khojastehnazhand^{a,*}, Hamed Ramezani^b

^a Department of Mechanical Engineering, Faculty of Engineering, University of Bonab, Bonab, P.BOX: 5551761167, Iran

^b Department of Biosystems Engineering, Faculty of Agricultural Engineering, Tarbiat Modares University, Tehran, Iran

ARTICLE INFO

Keywords:

Raisin
Texture
Feature
Classification
Image processing

ABSTRACT

Classification of bulk raisin is one of the main challenges to producers and buyers of raisin in the world. In this research, the quality of bulk raisin was investigated by using the image processing technique. For this purpose, 750 images of bulk raisin containing a different mixture of good and bad raisin with wood were used (50 images \times 15 class). Different texture feature algorithms combined with different modeling methods were used to evaluate the system performance. The study results showed that the Support Vector Machine (SVM) classifier using Gray Level Run Length Matrix (GLRM) features yielded more accurate classification results. The classification accuracy of modes I (6 classes of good and bad raisin) and II (15 classes) was obtained 85.55% and 69.78%, respectively. The results also indicated that the machine vision system could be used to classify good and bad raisin successfully, but in the case of mode II, it yielded weaker results.

1. Introduction

Raisin is one of the most important agricultural products in Iran which is obtained from grape drying. Iran is the world's second-largest raisin exporter after Turkey by producing 140,000 tons during 2017–2018 (Agricultural Statistics, 2017). Owing to the high moisture content of grapes and its corrosiveness, dried grapes (raisins) are usually used for long-term storage or export. Grape drying, in addition to prolonging its shelf life, reduces the effects of remaining pesticides on grapes (Cabras et al., 1997, 1998). One types of produced raisins is golden raisins produced using sulfur dioxide. The use of sulfur dioxide increases the drying rate and shelf life of the raisin. Since the produced raisin has impurities and waste such as wood and thistle, it is sold to any drying factories for any kind of cleaning process. In most cases, there is a challenge between the buyer and the seller to determine the quality of the product and the percentage of good, bad, and the amount of truffle and waste materials in the bulk raisin. Although the farmer tend to collect raisins with high moisture content without separation of bad raisins and thistles to get more profit, the factory manager has to make a decision on purchasing price based on the quality of raisins to avoid economic losses. Traditionally, bulk raisin quality is determined by experts based on personal experiences. This method is inaccurate, time-consuming and based on personal judgment. In recent decades,

with the development of science and technology, non-destructive optical methods have been widely used to determine the quality of agricultural products and foodstuffs such as apple (Unay et al., 2011; Yimyam and Clark, 2016), orange (Costa et al., 2009; Pham and Lee, 2015), wheat (Tahir et al., 2007; Guevara-Hernandez and Gomez-Gil, 2011) and weed (Granitto et al., 2002; Meyer et al., 1998). These methods have high accuracy, speed and reliability and can be applied to the entire product. Among non-destructive optical methods, we can refer to machine vision (Kazmi et al., 2015), spectroscopy (Pan et al., 2017) and hyperspectral imaging (Sun et al., 2017) methods. The machine vision method uses the RGB color space to extract the qualitative features of the product. The various qualitative characteristics, including color (Puerto et al., 2015), shape (Chen et al., 2010), texture (Burks et al., 2000) and spectra (Sun et al., 2017) properties can be considered to classify products. The texture features of products were used to detect damaged areas in apple or orange (Unay et al., 2011; Pham and Lee, 2015), weed detection (Burks et al., 2000), and seed purity for grain products such as wheat and rice (Guevara-Hernandez and Gomez-Gil, 2011). Different algorithms were used to evaluate and detect texture of agricultural products. Granitto et al. (2002) applied Gray Level Co-occurrence Matrix (GLCM) and Gray Level Run Length Matrix (GLRM) to classify weed seed. The classification accuracy of 99.2% was reported for test data set. In another research, GLCM and GLRM algorithms were used to grade wheat

* Corresponding author.

E-mail addresses: khojasteh@ubonab.ac.ir (M. Khojastehnazhand), hami_849@yahoo.com (H. Ramezani).

and barley grain (Guevara-Hernandez and Gomez-Gil, 2011). The classification accuracy levels of 98% and 68% for bulk grain and individual grain samples were reported, respectively. The quality and purity of the mixed raisin by using bulk raisin were evaluated by GLRM, GLCM and Local Binary Pattern (LBP) features (Karimi et al., 2017). They used only the mixture of good and bad raisin grain for imaging. The results of the proposed approach showed that the support vector machine (SVM) classifier yielded more efficient and accurate classification results than those obtained by artificial neural network (averagely 92.71%). However, in the real, the bulk raisin consisted of tails, thistle and waste materials. In this research, it was tried to evaluate different texture features to classify bulk raisin consisting of good and bad grains in addition to tails, thistle and waste materials.

2. Method and materials

Fig. 1 shows the overall flowchart of the current research. In this study, the samples were prepared from the different combinations of good and bad raisin along with tails, thistle and waste materials. The images of the samples were converted to gray-level images, and their textural features were extracted using Gray Level Co-occurrence Matrix (GLCM), Gray Level Run Length Matrix (GLRM) and Local Binary Pattern (LBP) methods. Linear Discriminate Analysis (LDA) and Support Vector Machine (SVM) as supervised classification methods and Principle Component Analysis as an unsupervised classification method were used to evaluate the features and comparison of the results. Eventually, the best model was introduced in terms of accuracy of class prediction. The whole process of image acquisition and texture features extraction was conducted in the MATLAB software environment. The modeling and result comparison of different methods were performed by using the Unscrambler X 10.4 program. In the following, all the research steps were explained in more details.

2.1. Sample preparation

10 kg golden raisin from a producer in Bonab region, Iran was purchased in December 2018. It was divided into three groups of good raisins, bad raisins and other waste materials. The good raisins were golden yellow raisins without any defects, however, bad raisins were black, wormy or rotten raisins and waste materials include thorns, shavings and plant leaves. A small dish with the dimensions of 50 mm × 50 mm and the height of 20 mm was used as a volume module to select from each of the above groups and to mix and form the classes to be considered. A total of 15 different classes were prepared based on various combinations of the mentioned three groups. To ensure that the raisins and woods were randomly placed in each class, they were first poured into a plastic bag and then by shaking the plastic bag, they were poured in a container with the dimensions of 150 mm × 150 mm and the height of 20 mm. The surface of the container was flattened manually and situated under the camera. Fig. 2 shows the images of 15 classes. The letter “G” represents the percentage of good raisins, the letter “B” indicates the percentage of bad raisins, and the letter “W” represents the percentage of wood in the class. For example, for creation of G50B30W20 class, 5 modules of good raisins, 3 modules of bad raisins and 2 modules of wood group were selected by small dish and then mixed completely by using a plastic bag. The mixed sample was poured in the container and the image of the sample was captured by machine vision system. In order to have random images of each class, the product was poured from the container into the plastic bag again and then by shaking it, poured into the container. This procedure was repeated 50 times for each class and 50 images were obtained.

2.2. Machine vision system

The machine vision system consists of a color camera, an

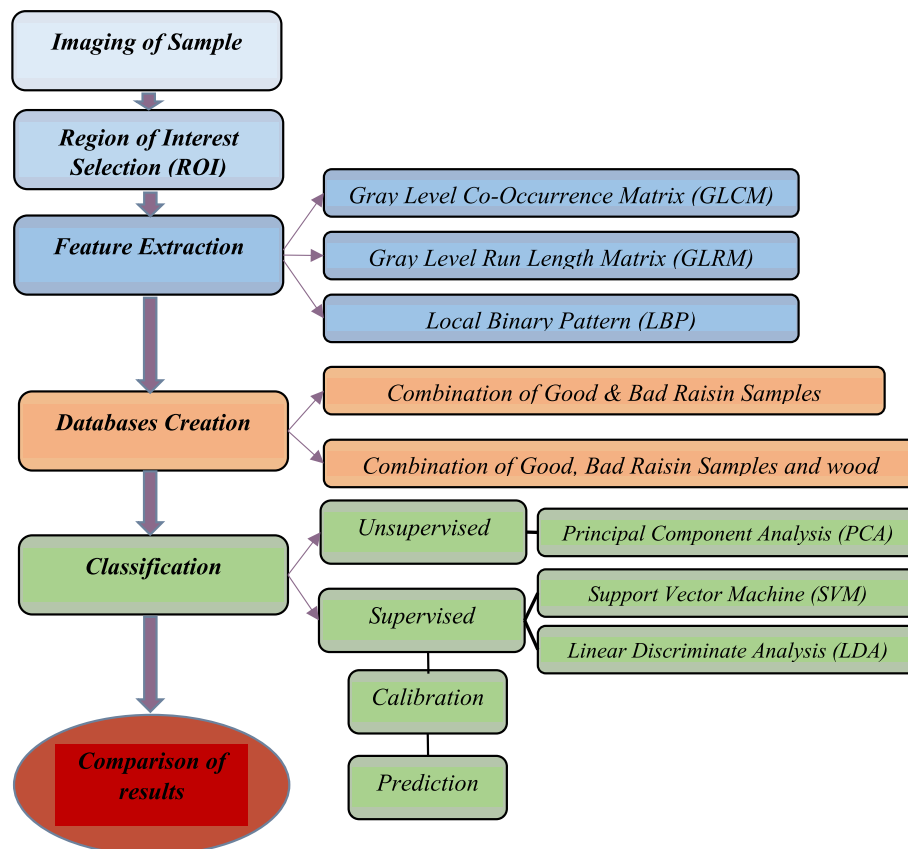


Fig. 1. Flowchart of bulk Raisin classification system using machine vision.

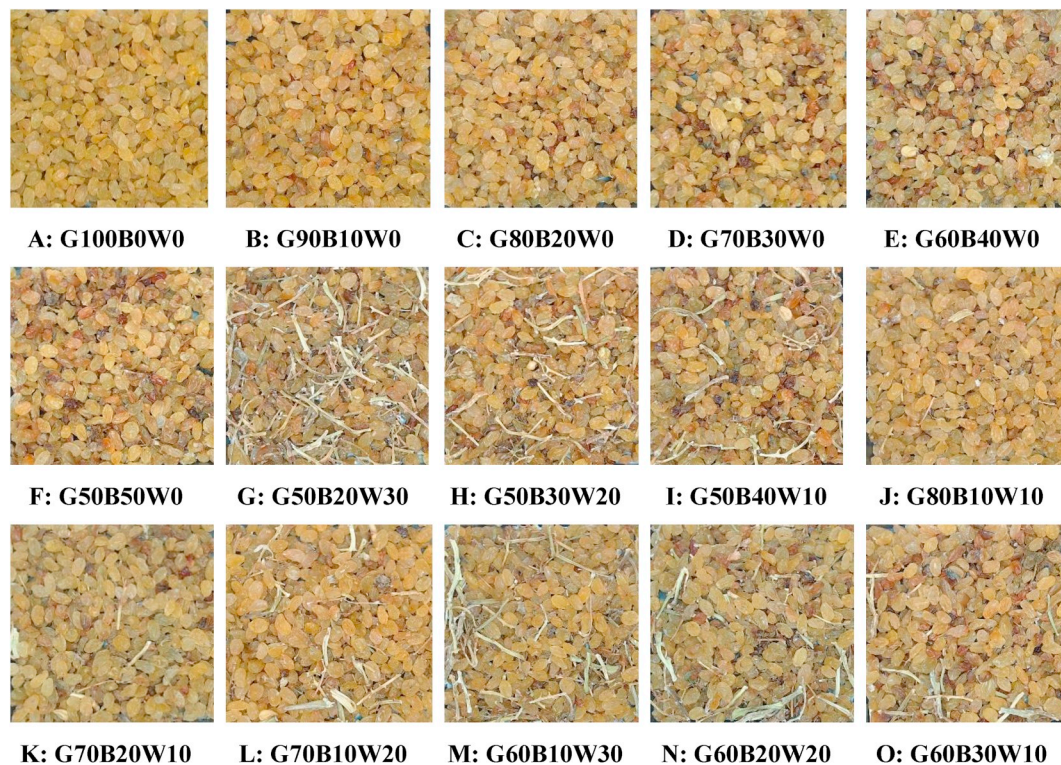


Fig. 2. The bulk raisin classes used for classification.

illumination system, a personal computer, and an imaging box. The imaging box was made of Medium-Density Fiberboard (MDF) in $40 \times 40 \times 50$ cm to eliminate the redundant lights and providing equal conditions of imaging for all 750 images (Fig. 3). Fig. 3 shows the installation location of the camera and the lighting system. The illumination system was a LED panel light (18 W) mounted around the camera. The color camera (CMOS Logitech C920 HD pro Webcam) with a resolution of 480×640 pixels and 30 frames per second was mounted on the center of the LED bulb ring with the height of 35 cm from the samples container and connected to the computer through a cable. The image of each class sample was taken and transferred to the computer for later processing.

2.3. Feature extraction

The quality of raisin product was evaluated based on its apparent texture. One of the useful methods to review the image is the use of a histogram. However, since the use of the histogram does not represent the distribution of different gray levels, GLCM, GLRM and LBP algorithms were used to study the distribution of gray levels. First, the provided images were cropped and then the three mentioned algorithms were used to extract texture features by turning the color image into a

gray image. For this purpose, a new matrix was first developed based on the distribution of gray levels, and the required properties for each matrix were extracted. By extracting the characteristics of each image, a complete database of all images and classes was created for the classification stage usage. The rows of the dataset matrix was based on the samples and the columns indicated the extracted features.

2.3.1. Gray level Co-occurrence matrix (GLCM)

A co-occurrence, referred to as co-occurrence distribution, is defined over an image to be the distribution of co-occurring values at occurring values at a given offset. In other words, GLCM represents the distance and angular spatial relationship over an image sub-region of a specific region. The GLCM is created from a gray-scale image and it calculates how often a pixel with gray-level (grayscale intensity or Tone) value i occurs either horizontally, vertically, or diagonally to adjacent pixels vertically, or diagonally with the value j (Majumdar and Jayas, 1999). After creation of the GLCM, several statistics such as energy, contrast, correlation and homogeneity can be derived from them by using different formulas (Table 1). These statistics provide information about the texture of an image. The energy of an image provides the sum of squared elements in GLCM. In addition, this feature is known as

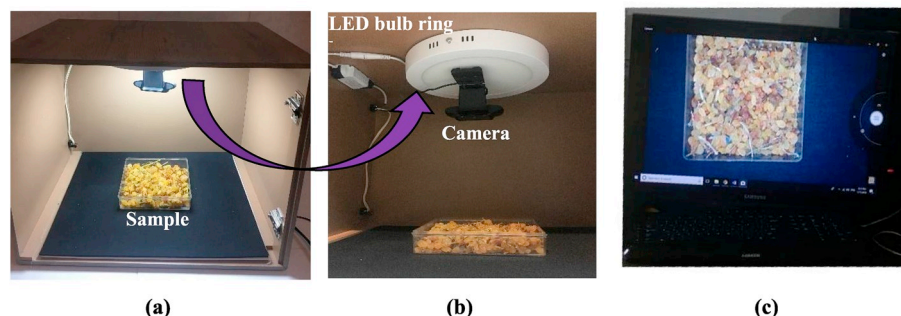


Fig. 3. Setup used for imaging; a) Imaging box; b) Upward view of the camera and LED bulb ring, c) PC monitor screen.

uniformity or angular second moment. Contrast measures the local variations in the gray-level co-occurrence matrix. Correlation measures the joint probability occurrence of the specified pixel pairs. Furthermore, homogeneity measures the closeness of the distribution of elements in the GLCM to GLCM diagonal. For each image, these statistics are calculated in 4 directions of 0, 45, 90 and 135. Therefore, for each image, 16 (4 features \times 4 directions) features were evaluated and used for classification.

Whereby $p(i, j)$ is normalized GLCM matrix, N_g is the number of gray levels in the GLCM, μ and σ are mean and variance of GLCM matrix.

2.3.2. Gray level run length matrix (GLRM)

The gray-level run length matrix (GLRLM) gives the size of homogeneous runs for each gray level. This matrix is computed for the 4 different directions and for each of the 11 texture indices derived from this matrix such as short run, long run, gray level non-uniformity, run length non-uniformity, run ratio, low gray level run, high gray level run, short run low gray level, short run high gray level, long run low gray level and Long run high gray level. The element (i, j) of GLRLM corresponds to the number of homogeneous runs of j pixels with intensity i in an image and is called GLRLM (i, j) thereafter. Table 2 shows the used 11 statistic features and their formulas. Considering the gray level run-length (GLRM) matrix, 11 features, including short run, long run, gray level non-uniformity, run ratio, run length non-uniformity, low gray level run, high gray level run, short run low gray level, short run high gray level, long run low gray level, and long run high gray level were extracted. For each image, 44 features (11 features \times 4 directions) were extracted.

Where $Q(i, j)$ is the GLRM matrix, i is the gray level value, j is the run length, and S is the sum of all values in the GLRM matrix.

2.3.3. Local binary pattern (LBP)

The third algorithm to extract the texture features of images was the local binary pattern method. LBP replaces the value of the pixels of an image with decimal numbers encoding the local structure around each pixel. By applying the LBP algorithm by using Matlab R2018a, a vector feature of every image was extracted and used in the modeling and classification stage.

2.4. Classification

Two supervised and unsupervised classification methods were used to classify the raisin classes. To investigate the accuracy of the classification models, the results were reported in 2 modes. Mode I was based on classification of 6 classes containing good and bad raisins. Mode II was based on classification of 15 classes containing good and bad raisin as well as wood. The principle component analysis (PCA) was used as an unsupervised classification method. PCA creates components to explain the observed variability in the predictor variables, without considering the response variable at all. In PCA, the first PC was plotted versus the second PC, since they contain the maximum variances among all the PCs. The score plot allows visualization of segregation and clustering among different classes. The ability for classification based on PCA was investigated visually. Additionally, Linear Discriminate Analysis (LDA) and Support Vector Machine (SVM) methods were used as supervised

Table 1
The features extracted from GLCM.

Feature	Equation
Energy	$\sum_i \sum_j p(i, j)^2$
Contrast	$\sum_{n=0}^{N_g-1} n^2 \{ \sum_{i=1}^{N_g} \sum_{j=1}^{N_g} p(i, j) \}, i-j =n$
Correlation	$\frac{\sum_i \sum_j (ij) p(i, j) - \mu_x \mu_y}{\sigma_x \sigma_y}$
Homogeneity	$-\sum_i \sum_j p(i, j) \log(p(i, j))$

Table 2

The features extracted from GLRM.

Feature	Equation
Short run	$\sum_i \sum_j (Q(i, j) / j^2) / S$
Long run	$\sum_i \sum_j (j^2 Q(i, j)) / S$
Gray level non-uniformity	$\sum_i (\sum_j Q(i, j))^2 / S$
Run length non-uniformity	$\sum_j (\sum_i Q(i, j))^2 / S$
Run ratio	$\sum_i \sum_j S / j Q(i, j)$
Low gray level run	$\sum_i \sum_j Q(i, j) / S i^2$
High gray level run	$\sum_i \sum_j i^2 Q(i, j) / S$
Short run low gray level	$\sum_i \sum_j Q(i, j) / S j^2 i^2$
Short run high gray level	$\sum_i \sum_j i^2 Q(i, j) / S j^2$
Long run low gray level	$\sum_i \sum_j j^2 Q(i, j) / S i^2$
Long run high gray level	$\sum_i \sum_j i^2 j^2 Q(i, j) / S$

methods. In the supervised classification methods, 35 samples randomly of each class (70% of samples) were used for calibration and 15 samples (30% of samples) were used for class prediction. The Squared Correlation Coefficient (R^2) of the predicted versus reference classes, Root Mean Squared Error (RMSE), sensitivity, specificity, and Correct Classification Rate (CCR) were used to evaluate the model.

2.5. Model evaluation

Sensitivity (Sen) and specificity (Spec) are two statistical parameters used along with correct classification rate (CCR) to evaluate the performance of a classification model. The sensitivity of Class A is the proportion of Class A (Positives) samples that classified as Class A (True Positive Rate). The specificity of Class A is the proportion of Class B (Negatives) samples which is classified as Class B (True Negatives Rate). These parameters can be written as Eqs. (1) and (2):

$$Sen = \frac{\text{Number of True Positives (TP)}}{\text{Number of Positives (P)}} = \text{Probability of Positive test} \quad (1)$$

$$Spec = \frac{\text{Number of True Negatives (TN)}}{\text{Number of Negatives (N)}} = \text{Probability of Negative test} \quad (2)$$

3. Results and discussion

3.1. PCA

Fig. 4 shows the principal component score plots for two modes I (6 classes) and II (15 classes). As PC1-PC2 plots show, the GLRM algorithm successfully classifies the 6 classes, while there is an overlap between the clusters of E and F that some samples of class E, classified as Class F. It is worth noting that the difference between the E and F classes is 10% of the raisin combination (bad and good) and an acceptable result has been achieved. In mode II, the results were weaker due to addition of wood and thistle to the samples, and none of the algorithms was able to perform well. GLRM algorithm has shown better performance compared to GLCM and LBP. The PC1 component covered more than 97% of the data. Among the reasons for the lack of accuracy in mode II, we can point out the color similarity of wood and thistle with good and bad raisins. Furthermore, due to the non-proportional size of the wood with raisins while distributing the sample container, good and bad raisins were not accepted with the wood uniformly, thereby they reduced the accuracy of the algorithm.

3.2. LDA and SVM

Table 3 shows the results of the classification using two supervised SVM and LDA models. The classification was performed by using the

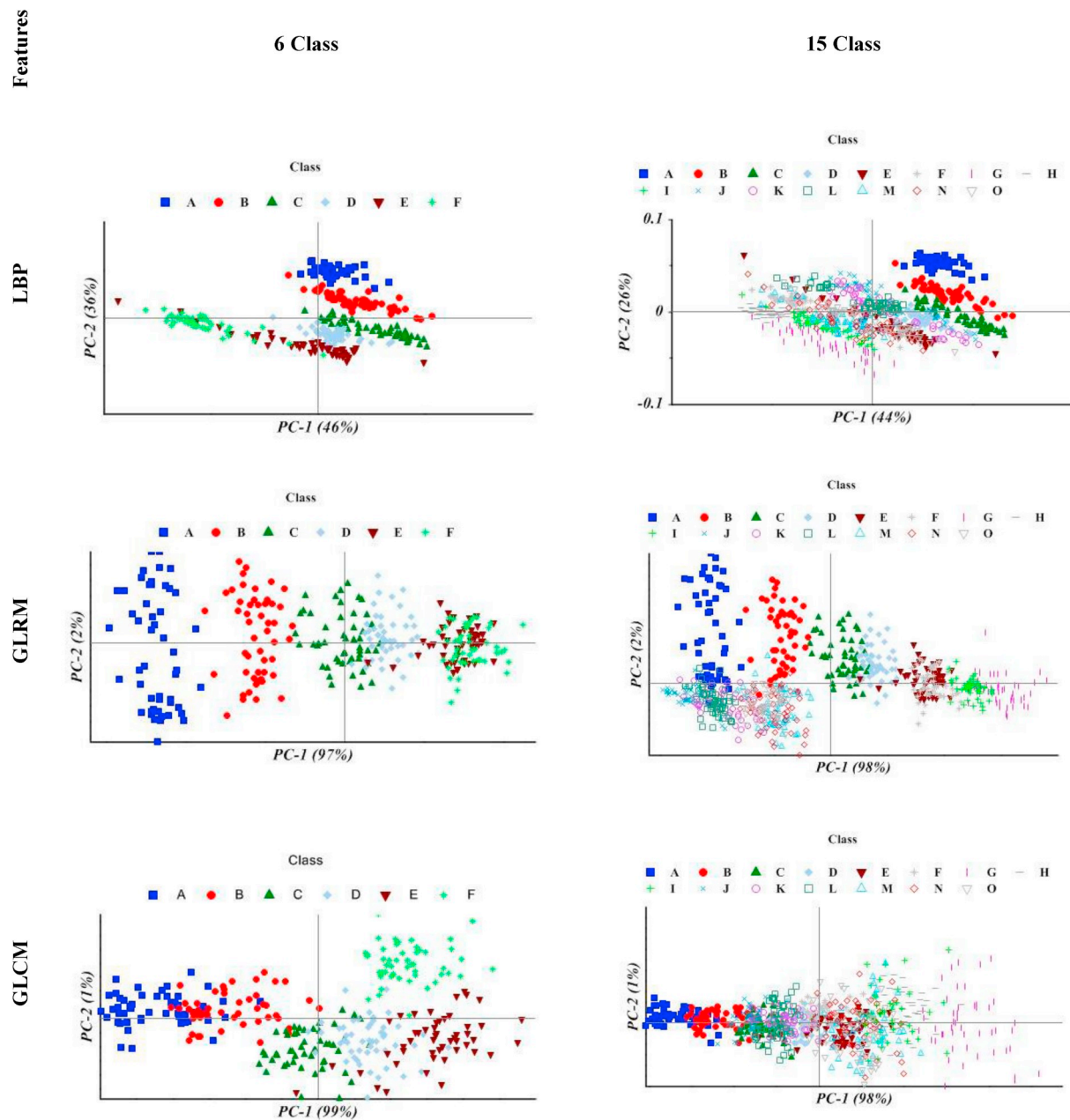


Fig. 4. The principal component score plots for two Modes I (6 classes) and II (15 classes).

features extracted by three GLCM, GLRM and LBP algorithms. As Table 3 shows, the GLRM algorithm for mode I has been able to operate with a prediction accuracy of 85.55% using the linear SVM model, which is the best result of the classification between the extracted features. Certainly, according to Table 3, despite the high predictive accuracy of the LDA Quadratic, since the linear SVM validation accuracy was higher than that, it was selected as the best model. Karimi et al. (2017) reported the ability of SVM model to classify the bulk raisin (good and bad raisins without wood). They reported that the performance of the SVM model was better than that of the artificial neural network model. In mode II, the linear SVM model had the highest accuracy and prediction accuracy based on GLRM features, which showed a prediction accuracy of 69.78%. A remarkable point in this table was the very weak SVM model results based on the LBP features that were not acceptable. This could be due to the feature vector provided by the LBP algorithm that could not be classified by SVM cluster planes. Concerning the results of mode II, the reasons for the weakness of the results were the color similarity of

the mixed wood in the sample with good and bad raisins, as well as inappropriate and random placement of wood due to the shape and size of the raisins. Tables 3 and 4 show the confusion matrix of the best result obtained for further investigation.

As Table 4 shows, the results obtained to detect the first three classes A, B, and C are acceptable, and the model is able to correctly identify the classes. However, for classes D and E, the results are weaker than those for the first three classes. It is noteworthy that according to the confusion matrix, for example, for class D, 8 samples were classified in class D and 6 in class E and 1 in class C. The class D: G70B30W0, is made up of 70% good raisin in combination with 30% percent bad raisin. However, class E: G60B40W0, is made up of 60% good raisin in combination with 40% percent bad raisin. Therefore, the differences between class D and E is 10%. This means that if a sample is incorrectly placed in one of the two classes, their content has 10% difference qualitatively.

The main reason for the poor result for D and E classes is the color variation of the bad raisins, including both dark and bright color raisin.

Table 3

The results of the classification using two supervised SVM and LDA models.

Features	Model		6 Class			15 Class		
			Cal	CV	Pre	Cal	CV	Pre
GLCM	SVM	Linear	88.1	84.24	84.44	72.95	68.19	63.55
		Polynomial	66.67	60.00	72.22	56.94	54.48	52.44
		Radial Basis	96.19	65.24	73.33	70.1	38.48	41.33
	LDA	Sigmoid	16.67	16.67	16.67	6.67	6.67	0.06
		Linear	84.29	83.55	82.22	44.76	43.68	42.22
		Quadratic	84.76	83.75	82.22	48.76	40.83	35.55
GLRM	SVM	Mahalanobis	85.24	80.18	77.78	46.48	44.23	41.78
		Linear	96.19	90.47	85.55	78.48	69.90	69.78
		Polynomial	98.1	92.86	83.33	67.43	63.29	62.22
	LDA	Radial Basis	0	0	0	0	0	0.06
		Sigmoid	16.67	16.67	16.67	6.67	6.67	0.06
		Linear	81.90	75.60	77.78	58.86	53.25	44.89
LBP	SVM	Quadratic	81.90	73.68	73.33	62.29	59.08	55.11
		Mahalanobis	82.86	70.74	71.11	62.29	58.96	52.89
	LDA	Linear	22.38	8.57	14.44	2.10	4.76	0.02
		Polynomial	32.38	16.67	32.22	13.33	6.67	13.33
		Radial Basis	25.24	16.67	16.67	13.14	6.67	13.33
		Sigmoid	25.24	16.67	16.67	13.33	6.67	13.33
	LDA	Linear	91.43	88.26	97.78	63.43	62.95	62.67
		Quadratic	92.86	89.56	96.67	67.05	66.80	65.78
		Mahalanobis	92.86	89.54	96.67	67.76	63.54	59.11

Table 4

The confusion matrix of bulk raisin classification using GLRM features and linear SVM model for 6 class (Mode I).

Class	A	B	C	D	E	F
A	14	1	0	0	0	0
B	0	15	0	0	0	0
C	0	0	14	1	0	0
D	0	0	1	8	6	0
E	0	0	0	2	12	1
F	0	0	0	1	0	14
Sen	93.33	100	93.33	53.33	80.00	93.33
Spec	98.66	98.66	98.66	94.66	92.00	98.66
CCR	100	93.75	93.33	66.67	66.67	93.33

The color variation does not significantly affect the precision in the first three classes (A, B and C) owing to their low percentage of total product, but significantly affects grades D and E. The classification accuracy of class F is acceptable as in classes A, B, and C. The observed results in the classifications are consistent with those of observation in the PC1-PC2 plot and are validated by each other. Karimi et al. (2017) also achieved similar results in one study into good and bad raisins mixture.

The confusion matrix for mode II is slightly different from that of

mode I. The sensitivity, specificity and CCR values for the first six classes are acceptable, except for classes D and E, and are similar to the results of mode I. However, weaker results are observed for the subsequent classes, including wood and thistle in the samples (Table 5). Certainly, it can be observed that the values obtained in all classes are written in a diagonal form, indicating that if the sample is classified incorrectly, it is in the class before or after it has taken. In other words, since the class content is only 10% in terms of content in the composition, the machine vision system has been able to identify the nearest class to the class with a partial error. As Fig. 3 clearly shows, in the case of class I having zero accuracy, this class is visually similar to other classes. This is due to the different shape of the wood and thistle from raisin seeds. Despite of mixing them before imaging, the location of the wood is different, thereby reducing the accuracy of the woody samples.

4. Conclusion

Raisin is one of the most important dried fruits in Iran and annual production in Iran is 140000 tons. In addition to other challenges in the planting, harvesting and processing of the raisin in the farm, the main challenge is between the producer and the buyer of dried raisin to choose the fees of the product. The machine vision system was used to

Table 5

The confusion matrix of bulk raisin classification using GLRM features and linear SVM model for 15 class (Mode II).

Class	A	B	C	D	E	F	G	H	I	J	K	L	M	N	O
A	15	0	0	0	0	0	0	0	0	0	0	0	0	0	0
B	0	15	0	0	0	0	0	0	0	0	0	0	0	0	0
C	0	0	14	1	0	0	0	0	0	0	0	0	0	0	0
D	0	0	1	8	6	0	0	0	0	0	0	0	0	0	0
E	0	0	0	1	14	0	0	0	0	0	0	0	0	0	0
F	0	0	0	0	1	14	0	0	0	0	0	0	0	0	0
G	0	0	0	0	0	0	12	3	0	0	0	0	0	0	0
H	0	0	0	0	0	4	0	11	0	0	0	0	0	0	0
I	0	0	0	0	0	5	0	10	0	0	0	0	0	0	0
J	0	0	0	0	0	0	0	0	0	12	0	3	0	0	0
K	0	0	0	0	0	0	0	0	0	2	7	6	0	0	0
L	0	0	0	0	0	0	0	0	0	2	1	12	0	0	0
M	0	0	0	0	0	0	0	0	0	0	1	0	7	7	0
N	0	0	0	0	0	0	0	0	0	0	1	0	5	8	1
O	0	0	0	0	0	0	0	0	0	0	0	0	1	7	7
Sen	100	100	93.33	53.33	93.33	93.33	80.00	73.33	0.00	80.00	46.67	80.00	46.67	53.33	46.67
Spec	100	100	99.52	99.04	96.67	95.71	100	93.80	100	98.09	98.57	95.71	97.14	93.33	99.52
CCR	100	100	93.33	80.00	66.67	60.87	100	45.83	0	75.00	70.00	57.14	53.84	36.36	87.50

extract the quality attributes of the samples using GLCM, GLRM and LBP features. The results showed that the SVM model had better performance than the LDA model. The obtained results were confirmed by the PC plot as an unsupervised method. The mixture of tails, thistle and waste materials with the good and bad raisins decreased the system performance. However, the misclassified samples, usually classified in the nearest class, showed that acceptable results were obtained. The results could be used to design quality measurement of bulk raisin that producers, buyers and sellers can use it. Future research can be conducted on detection of tails, thistle and waste materials before detecting good and bad raisins in order to enhance the system's performance accuracy. Future work will include using other modeling techniques such as genetic algorithm and artificial neural network to optimize the results, as well as extract some other texture features of the samples.

Credit author statement

Mostafa Khojastehnazhand: Methodology, Data Curation, Formal analysis, Writing - Original Draft, Writing - Review & Editing, Supervision. **Hamed Ramezani:** Conceptualization, Methodology, Software, Writing - Original Draft.

Acknowledgment

This work was supported by the deputy of research of University of Bonab "Grant no: 96/D/AP/1914, 2018" and the authors would like to express their sincere thanks to their technical and financial support.

References

- Agricultural Statistics, 2017. Ministry of agriculture, deputy director of economic and planning, ICT center. Retrieved from. <https://usda.library.cornell.edu>. (Accessed 20 December 2018).
- Burks, T., Shearer, S., Payne, F., 2000. Classification of weed species using color texture features and discriminant analysis. *Trans. ASAE (Am. Soc. Agric. Eng.)* 43 (2), 441.
- Cabras, P., Angioni, A., Garau, V.L., Minelli, E.V., Cabitza, F., Cubeddu, M., 1997. Residues of some pesticides in fresh and dried apricots. *J. Agric. Food Chem.* 45, 3221–3222.
- Cabras, P., Angioni, A., Garau, V.L., Melis, M., Pirisi, F.M., Cabitza, F., Pala, M., 1998. Pesticide residues in raisin processing. *J. Agric. Food Chem.* 46 (6), 2309–2311.
- Chen, X., Xun, Y., Li, W., Zhang, J., 2010. Combining discriminant analysis and neural networks for corn variety identification. *Comput. Electron. Agric.* 71, S48–S53.
- Costa, C., Menesatti, P., Paglia, G., Pallottino, F., Aguzzi, J., Rimatori, V., Recupero, G.R., 2009. Quantitative evaluation of tarocco sweet orange fruit shape using optoelectronic elliptic fourier based analysis. *Postharvest Biol. Technol.* 54 (1), 38–47.
- Granitto, P.M., Navone, H.D., Verdes, P.F., Ceccatto, H., 2002. Weed seeds identification by machine vision. *Comput. Electron. Agric.* 33 (2), 91–103.
- Guevara-Hernandez, F., Gomez-Gil, J., 2011. A machine vision system for classification of wheat and barley grain kernels. *Span. J. Agric. Res.* 9 (3), 672–680.
- Karimi, N., Kondrood, R.R., Alizadeh, T., 2017. An intelligent system for quality measurement of Golden Bleached raisins using two comparative machine learning algorithms. *Measurement* 107, 68–76.
- Kazmi, W., Garcia-Ruiz, F.J., Nielsen, J., Rasmussen, J., Andersen, H.J., 2015. Detecting creeping thistle in sugar beet fields using vegetation indices. *Comput. Electron. Agric.* 112, 10–19.
- Majumdar, S., Jayas, D.S., 1999. Classification of bulk samples of cereal grains using machine vision. *J. Agric. Eng. Res.* 73 (1), 35–47.
- Meyer, G., Mehta, T., Kocher, M., Mortensen, D., Samal, A., 1998. Textural imaging and discriminant analysis for distinguishing weeds for spot spraying. *Trans. ASAE (Am. Soc. Agric. Eng.)* 41 (4), 1189.
- Pan, L., Sun, Y., Xiao, H., Gu, X., Hu, P., Wei, Y., Tu, K., 2017. Hyperspectral imaging with different illumination patterns for the hollowness classification of white radish. *Postharvest Biol. Technol.* 126, 40–49.
- Pham, V.H., Lee, B.R., 2015. An image segmentation approach for fruit defect detection using k-means clustering and graph-based algorithm. *Vietnam J. Comput. Sci.* 2 (1), 25–33.
- Puerto, D.A., Gila, D.M.M., García, J.G., Ortega, J.G., 2015. Sorting olive batches for the milling process using image processing. *Sensors* 15 (7), 15738–15754.
- Sun, Y., Gu, X., Sun, K., Hu, H., Xu, M., Wang, Z., Pan, L., 2017. Hyperspectral reflectance imaging combined with chemometrics and successive projections algorithm for chilling injury classification in peaches. *LWT - Food Sci. Technol. (Lebensmittel-Wissenschaft -Technol.)* 75, 557–564.
- Tahir, A., Neethirajan, S., Jayas, D., Shahin, M., Symons, S., White, N., 2007. Evaluation of the effect of moisture content on cereal grains by digital image analysis. *Food Res. Int.* 40 (9), 1140–1145.
- Unay, D., Gosselin, B., Kleynen, O., Leemans, V., Destain, M., Debeir, O., 2011. Automatic grading of bi-colored apples by multispectral machine vision. *Comput. Electron. Agric.* 75 (1), 204–212.
- Yimyan, P., Clark, A.F., 2016. 3D reconstruction and feature extraction for agricultural produce grading. In: Paper Presented at the Knowledge and Smart Technology (KST), 2016 8th International Conference on, pp. 136–141.